Cell Reports

Article

JAML immunotherapy targets recently activated tumor-infiltrating CD8$^+$ T cells

Graphical abstract

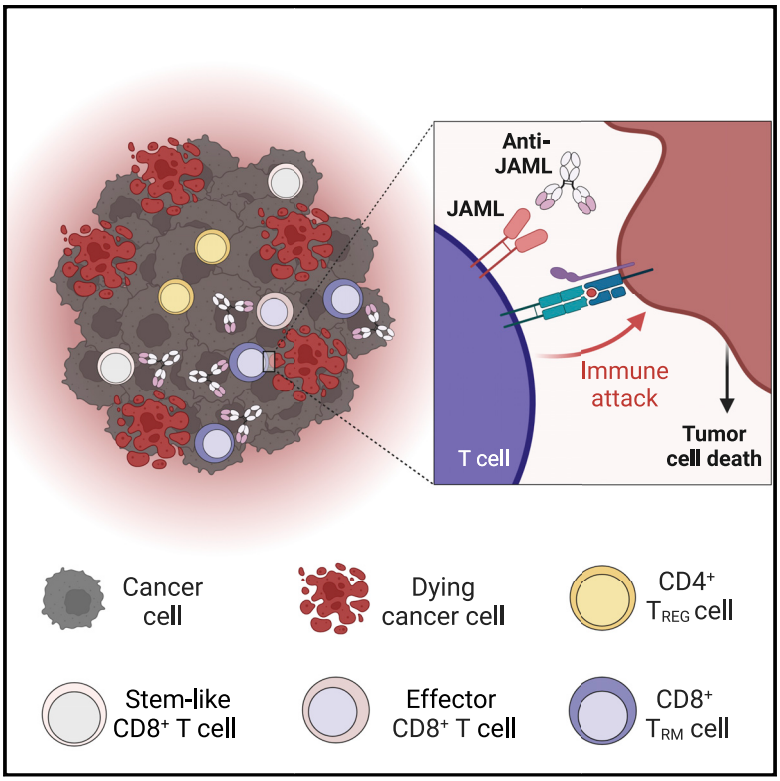

Authors

Simon Eschweiler, Alice Wang, Ciro Ramírez-Suástegui, ..., Vivek Chandra, Christian H. Ottensmeier, Pandurangan Vijayanand

Correspondence

vijay@lji.org

In brief

Eschweiler et al. identify JAML as a promising immunotherapy target with low on-target/off-cell and on-target/off-tumor effects. When compared with other immunotherapy targets plagued by low target specificity and end-organ toxicity, they find JAML to be mostly restricted to and highly expressed by (tissue-resident) CD8$^+$ T cells in multiple cancer types.

Highlights

- JAML is a co-stimulatory molecule in human and murine αβ T cells
- JAML is induced by TCR stimulation and enriched in tumor-infiltrating T_{RM} cells
- JAML expression in T_{RM} cells is associated with better survival outcomes in HNSCC
- Agonistic anti-JAML controls tumor growth and synergizes with anti-PD-1 therapy

Eschweiler et al., 2023, Cell Reports *42*, 112040
February 28, 2023
https://doi.org/10.1016/j.celrep.2023.112040

CellPress

Cell Reports

CellPress
OPEN ACCESS

Article

JAML immunotherapy targets recently activated tumor-infiltrating CD8$^+$ T cells

Simon Eschweiler,[1] Alice Wang,[1] Ciro Ramírez-Suástegui,[1] Adrian von Witzleben,[2] Yingcong Li,[1,3] Serena J. Chee,[4,5] Hayley Simon,[1] Monalisa Mondal,[1] Matthew Ellis,[6,7] Gareth J. Thomas,[6,7] Vivek Chandra,[1] Christian H. Ottensmeier,[1,4,8] and Pandurangan Vijayanand[1,3,4,8,9,*]

[1]La Jolla Institute for Immunology, La Jolla, CA, USA
[2]Department of Otorhinolaryngology, Head and Neck Surgery, Ulm University Medical Center, Ulm, Germany
[3]University of California San Diego, La Jolla, CA, USA
[4]Department of Molecular and Clinical Cancer Medicine and NIHR and CRUK Liverpool Experimental Cancer Medicine Center, University of Liverpool, Liverpool, UK
[5]Department of Respiratory Medicine, Liverpool Heart and Chest Hospital and NHS Foundation Trust, Liverpool, UK
[6]NIHR and CRUK Southampton Experimental Cancer Medicine Center, Faculty of Medicine, University of Southampton, Southampton, UK
[7]NIHR Southampton Biomedical Research Center, Faculty of Medicine, University of Southampton, Southampton, UK
[8]These authors contributed equally
[9]Lead contact
*Correspondence: vijay@lji.org
https://doi.org/10.1016/j.celrep.2023.112040

SUMMARY

Junctional adhesion molecule-like protein (JAML) serves as a co-stimulatory molecule in γδ T cells. While it has recently been described as a cancer immunotherapy target in mice, its potential to cause toxicity, specific mode of action with regard to its cellular targets, and whether it can be targeted in humans remain unknown. Here, we show that JAML is induced by T cell receptor engagement, reveal that this induction is linked to *cis*-regulatory interactions between the *CD3D* and *JAML* gene loci. When compared with other immunotherapy targets plagued by low target specificity and end-organ toxicity, we find JAML to be mostly restricted to and highly expressed by tissue-resident memory CD8$^+$ T cells in multiple cancer types. By delineating the key cellular targets and functional consequences of agonistic anti-JAML therapy in a murine melanoma model, we show its specific mode of action and the reason for its synergistic effects with anti-PD-1.

INTRODUCTION

Immunotherapies targeting co-stimulatory or co-inhibitory receptors on T cells have become an important treatment option for a variety of cancer types, and several molecules like TIM3,[5] TIGIT,[6] GITR,[7] VISTA,[8] LAG3,[9] or ICOS[10] are currently being explored to evaluate their anti-tumor capacity. Crucially, however, most of these targets suffer from "on-target/off-cell" effects, as both effector and regulatory T cell subsets in tumor tissues can express high levels of these molecules. Accordingly, we have recently shown that intratumoral PD-1 expressing follicular regulatory T (T_{FR}) cells are critical determinants of anti-PD-1 treatment efficacy, and that anti-PD-1 therapy can activate such suppressive cells, thus dampening treatment efficacy.[11] In line with this, it has been demonstrated that the balance of PD-1 expressing CD8$^+$ T cells and T regulatory (T_{REG}) cells in the tumor microenvironment (TME) is a critical biomarker predicting anti-PD-1 treatment efficacy.[12] Furthermore, we[13,4] and others[14–16] have demonstrated the critical importance of CD8$^+$ T_{RM} cells for anti-tumor immunity in multiple cancer types, and, while they have also been shown as being specific for tumor antigens,[16] so far, immunotherapies that preferentially target T_{RM} cells have not been described. These findings imply that expression levels of immunotherapy targets on different T cell subsets need to be carefully evaluated to determine which patients might benefit from a given treatment. Furthermore, while established immunotherapy drugs like anti-PD-1 or anti-CTLA-4 have shown remarkable success in some instances, only a fraction (∼20%) of patients respond to treatment.[17] It is well appreciated that anti-CTLA-4/anti-PD-1 combination therapy results in significantly higher overall response rates compared with monotherapy with either agent, but that combination therapy also induces more frequent and severe immune-related adverse events (irAEs) due to "on-target/off-tumor" effects on T cells present in normal tissues, thus limiting its use.[18] Because off-cell effects and widespread immune-related toxicity severely limit both treatment efficacy and combination therapy options, there is urgent need to develop novel immunotherapy targets that exhibit a more restricted expression profile.

JAML was initially identified as the major co-stimulatory molecule in epithelial γδ T cells, and activation by coxsackie and adenovirus receptor (CXADR), its ligand expressed by epithelial cells, has been shown to be important for tissue homeostasis and wound repair.[19,20] While JAML has an overall low sequence identity with the co-stimulatory molecule CD28 (∼11%), its intracellular signaling motifs bear substantial similarities and, upon ligation, recruit phosphatidylinositol-3-OH-kinase (PI3K), leading

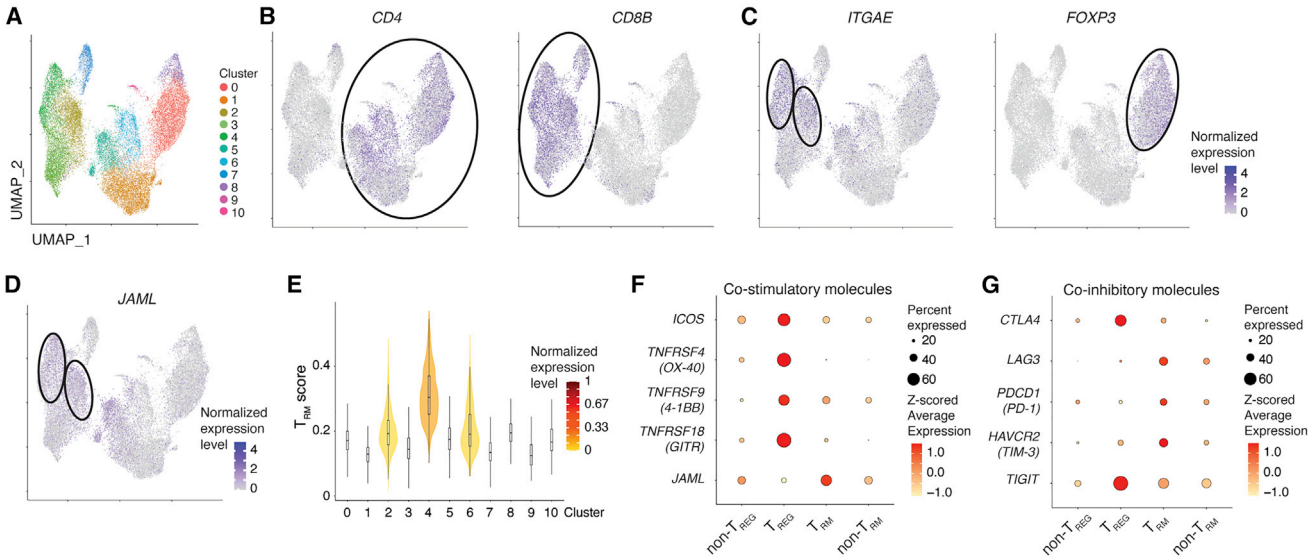

Figure 1. JAML is enriched in tumor-infiltrating CD8$^+$ T_{RM} cells of multiple cancer types

(A–D) Integrated analysis of nine published single-cell RNA-seq datasets from six different cancer types visualized by UMAP depicting CD4 and CD8 T cells (A). Seurat-normalized expression of *CD4* (B, left), *CD8B* (B, right), *ITGAE* (C, left), *FOXP3* (C, right), and *JAML* (D) in the different clusters.

(E) Identification of T_{RM} clusters using a previously published intratumoral T_{RM} gene signature.

(F and G) Average transcript expression (color) and percentage (size) for selected co-stimulatory (F) and co-inhibitory (G) molecules in non-T_{REG}, T_{REG}, T_{RM}, and non-T_{RM} cells for integrated analysis (A–D).

to cell activation, proliferation, and cytokine production.[19,20] Moreover, in mouse models, JAML has been implicated as an appealing cancer immunotherapy target.[21]

However, its role and function in tumor-infiltrating human αβ T cells, especially T_{RM} cells, remain unexplored. Here, we report that JAML functions as a co-stimulatory molecule in human αβ CD8$^+$ T cells, and that its expression is increased by TCR signaling. Using 3D chromatin interaction maps in human T cells, we demonstrate extensive interactions between the *JAML* promoter and the neighboring *CD3D* promoter region driving *JAML* expression in activated T cells, but not other cell compartments. Analysis of transcriptomes and protein expression data in tumor-infiltrating lymphocytes (TILs) from multiple cancer types in humans show that JAML is highly expressed by CD8$^+$ T_{RM} cells and that JAML expression on CD8$^+$ T_{RM} cells is associated with better survival outcomes in a large cohort of head and neck squamous cell carcinoma patients. Finally, in a murine melanoma model, we confirmed restricted expression of JAML on CD8$^+$ T cells in primary tumor tissue, but not other non-malignant organs. Crucially, we found JAML to be expressed on distinct "stem-like" *Tcf7*^{hi}*Pdcd1*^{lo} and cytotoxic *Pdcd1*^{hi}*Tcf7*^{lo} CD8$^+$ TIL subsets, that, together with our unbiased RNA sequencing (RNA-seq) data, uncover why anti-JAML acts synergistically with anti-PD-1 therapy to augment TIL infiltration and anti-tumor immunity.

RESULTS

JAML is enriched in tumor-infiltrating CD8$^+$ T_{RM} cells of multiple cancer types

As few studies have thoroughly assessed the level and breadth of immunotherapy target expression in T cell subsets in the TME, we integrated and analyzed nine published single-cell RNA-seq datasets of tumor-infiltrating CD4$^+$ and CD8$^+$ T cells (n = 22,410 cells) spanning seven different cancer types. Data visualization using uniform manifold approximation and projection (UMAP) revealed 10 distinct T cell subsets (Figures 1A–1C) that differed substantially in their expression of several co-stimulatory and co-inhibitory receptors (Figure S1A). We verified that the main clusters were not dominated by cells from individual datasets; only clusters with few cells (9 and 10) seemed to divert from that trend (Figure S1B). Given the opposing roles of CD4$^+$FOXP3$^+$ (T_{REG}) cells and CD8$^+$ T_{RM} cells in anti-tumor immunity and immunotherapy efficacy,[11,13,15,22–26] we assessed the transcript expression levels of several immunotherapy targets in these major CD4$^+$ (non-T_{REG} and T_{REG}) and CD8$^+$ (T_{RM} and non-T_{RM}) T cell subsets and verified cell identify of T_{RM} cells by using a previously published tumor T_{RM} gene signature[4] (Figures 1B–1G). Importantly, T_{REG} cells, when compared with the other T cell subsets, expressed higher levels of transcripts encoding for several co-stimulatory and co-inhibitory immunotherapy drug targets currently in clinical use or clinical trials (e.g., 4-1BB, ICOS, OX-40, GITR, TIGIT) (Figures 1F and 1G), while some co-inhibitory receptors were expressed on all assessed T cell subsets (Figure 1G). On the other hand, we found *JAML* transcripts to be expressed at relatively higher levels by CD8$^+$ T_{RM} cells when compared with T_{REG} cells (Figure 1F). Because co-stimulatory molecules enhance TCR-dependent cell activation, proliferation, and effector functions, we next tested whether *JAML*-expressing T cells exhibit transcriptional features of superior functionality when compared with their *JAML*-non-expressing counterparts. Notably, we found that *JAML*-expressing T_{RM} cells expressed higher levels of

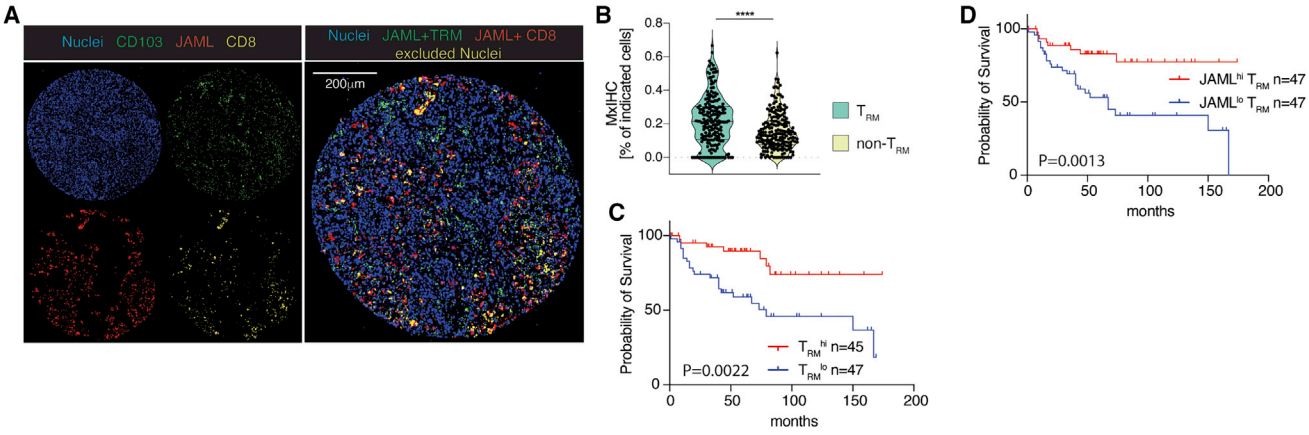

Figure 2. JAML expression on T_{RM} cells is associated with patient survival

(A) Whole-slide multiplexed immunohistochemistry analysis of selected markers from a treatment-naïve patient with NSCLC.

(B) Whole-slide multiplexed immunohistochemistry analysis depicting the percentage of JAML-expressing $CD8^+$ T_{RM} ($CD8^+CD103^+$) and $CD8^+$ non-T_{RM} ($CD8^+CD103^-$) cells in the cohort of HNSCC patients.

(C and D) Survival curves of an HNSCC cohort (n = 194) stratified into T_{RM}^{hi} and T_{RM}^{lo} (C), $JAML^{hi}$ and $JAML^{lo}$ T_{RM} cells (D). All data are mean ± SEM. Significance for comparisons was computed using two-tailed Wilcoxon matched-pairs signed rank test (B) or Mantel-Cox test (C and D), p = 0.1234; *p = 0.0332; **p = 0.0021; ***p = 0.0002; and ****p < 0.0001.

transcripts encoding for cytotoxicity molecules (Granzyme B, Perforin) and effector cytokines (IFN-γ, CXCL13) when compared with T_{RM} cells not expressing *JAML* (Figure S1C), suggesting that JAML expression marks T_{RM} cells with enhanced functional properties, or that JAML itself enhances functionality. Given that the expression pattern of co-stimulatory and co-inhibitory receptors was observed in many cancer types, we next verified immunotherapy target protein expression levels on tumor-infiltrating T_{REG} and $CD8^+$ T cells in patients with early-stage and treatment-naïve non-small cell lung cancer (NSCLC) (Figure S1D). These analyses corroborated our findings from single-cell RNA-seq data and confirmed that several immunotherapy target molecules are expressed at higher levels by tumor-infiltrating T_{REG} cells.

Together, these data suggest that immune-suppressive T_{REG} cells can get activated by agonistic antibodies targeting co-stimulatory molecules or by antibodies blocking co-inhibitory molecules, thus dampening their treatment efficacy. Conversely, JAML is primarily expressed by $CD8^+$ T_{RM} cells, implying that agonistic anti-JAML antibodies would preferentially activate $CD8^+$ T_{RM} cells with superior functionality and thus augment anti-tumor immunity.

JAML expression on T_{RM} cells is associated with improved survival outcomes

Based on these data and given that we found that *JAML* is primarily expressed on highly functional T_{RM} cells in tumor tissues,[4] we reasoned that expression of JAML in T_{RM} cells may positively influence their anti-tumor activity and thus survival outcomes, and examined such association in a large cohort of patients with head and neck squamous cell carcinoma (HNSCC) (n = 194). As expected, we found that a greater proportion of $CD8^+$ T_{RM} cells expressed JAML when compared with $CD8^+$ non-T_{RM} cells (Figures 2A and 2B). Consistent with previous reports in NSCLC[13] or early-stage triple-negative breast cancer,[14] we demonstrate that intratumoral density of $CD8^+$ T_{RM} cells is significantly associated with improved patient survival (Figure 2C). Moreover, HNSCC patients with higher proportions of JAML-expressing $CD8^+$ T_{RM} cells in the tumor had significantly better long-term overall survival outcomes when compared with those with lower proportions of JAML-expressing T_{RM} cells ($JAML^{low}$ T_{RM} tumors) (Figure 2D). These results suggest that expression of JAML is likely to confer T_{RM} cells with enhanced anti-tumor activity.

JAML functions as a co-stimulatory signal in human αβ T cells

As previous studies implied that JAML might not function as a co-stimulatory molecule in αβ T cells,[19,20] we tested whether ligand binding to JAML triggers activation of human $CD4^+$ and $CD8^+$ T cells. At a sub-optimal concentration (0.5 μg/mL) of anti-CD3, which by itself did not induce cell activation (Figure S2A), JAML ligation by its endogenous ligand CXADR led to rapid and dose-dependent upregulation of the early activation markers CD69, CD25, PD-1, and 4-1BB (Figure S2B) and cell proliferation (Figure S2C). Even at low concentrations, we found that JAML, like the co-stimulatory molecule CD28, potently activated $CD4^+$ and $CD8^+$ T cells (Figure S2B). To confirm that CXADR activates T cells through ligation of JAML, we knocked down JAML expression in primary human $CD8^+$ T cells by using Crispr-Cas9 and assessed co-stimulatory effects of CXADR. Transfection of $CD8^+$ T cells with a JAML guide RNA altered the nucleotide sequence in the targeted JAML gene region (Exon 2), presumably driven by CRISPR-Cas9-mediated insertion or deletion events (Figure S3A), significantly diminished *JAML* expression (Figure S3B), and reduced T cell activation and cytokine secretion by CXADR co-stimulation (Figures S3C and S3D). Contrary to the previous report,[20] these data demonstrate that JAML facilitates potent co-simulation in αβ T cells.

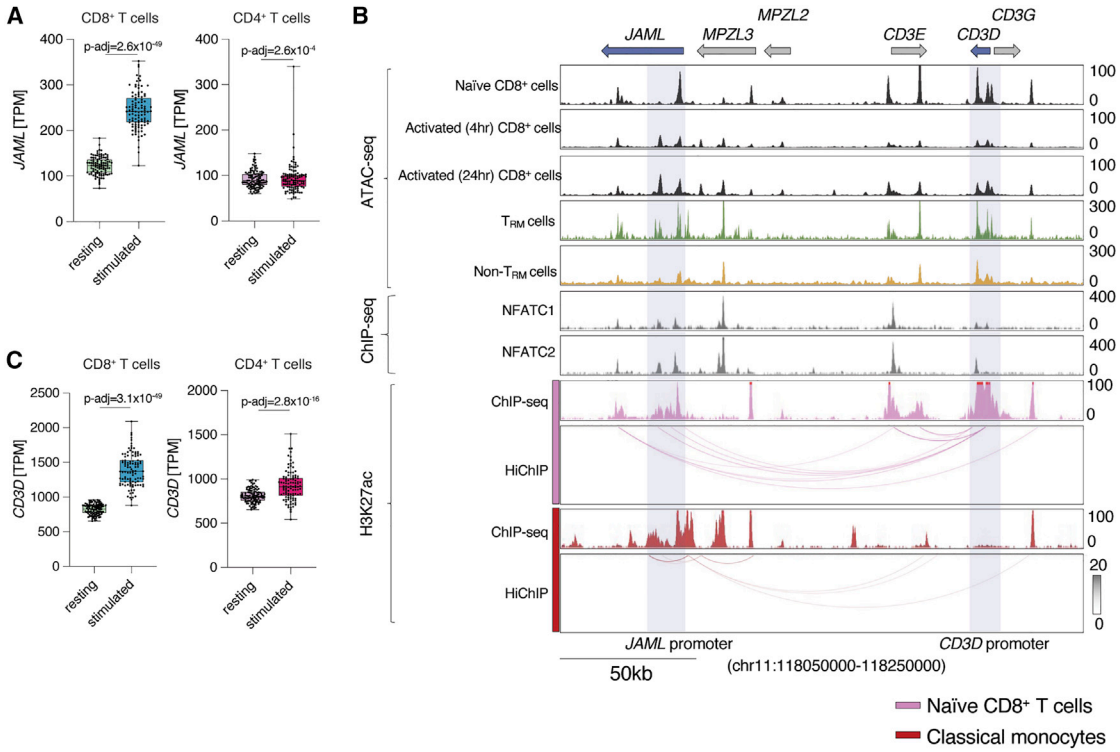

Figure 3. JAML expression is induced by *cis*-regulatory interactions between the *CD3D* and *JAML* promoters

(A) *JAML* expression (TPM) in resting and anti-CD3 and anti-CD28-stimulated CD4$^+$ and CD8$^+$ T cells from donors (n = 104) from a published bulk RNA-seq dataset.[1]

(B) ATAC-seq, chromatin immunoprecipitation (ChIP)-seq tracks, and HiChIP interactions for the extended *JAML* and *CD3* gene loci in indicated cell populations; the black arrow indicates the activation-induced intronic region.

(C) *CD3D* expression (TPM) in resting and anti-CD3 and anti-CD28-stimulated CD4$^+$ and CD8$^+$ T cells from donors (n = 104) from a published bulk RNA-seq dataset.[1]

JAML expression is regulated by interactions between the *CD3D* and *JAML* promoters

Using our previously published dataset,[1] we found that TCR stimulation more significantly increased *JAML* expression in human CD8$^+$ T cells compared with CD4$^+$ T cells (log_2 fold change 1.24 versus 0.37 in CD8$^+$ and CD4$^+$ T cells, respectively; Figure 3A). To investigate how TCR signaling induces *JAML* expression in $\alpha\beta$ T cells, we first examined transposase accessible regions (ATAC-seq peaks) in the *JAML* locus in resting and stimulated human CD8$^+$ and CD4$^+$ T cells (Figures 3B and S4A). Activation induced a strong ATAC-seq peak in the *JAML* intronic region (Figure 3B) that also contained binding sites for NFAT, a key transcription factor involved in activation of genes following TCR activation. Notably, human tumor-infiltrating T_{RM} cells displayed greater accessibility at the *JAML* promoter and the pertaining activation-induced intronic ATAC-seq peak region when compared with non-T_{RM} cells. We also found several NFAT binding sites in the promoter regions of upstream genes like *CD3D* and *CD3G* that encode for key components of the TCR, and that like JAML, showed increased expression following activation (Figure 3B). Importantly, by examining the 3D chromatin interaction map of the extended *JAML* locus in primary human T cells,[2] we found that the *JAML* promoter and the activation-induced intronic *cis*-regulatory region strongly interacted with the neighboring *CD3D* promoter region (Figure 3B), suggesting that they are likely to be involved in regulating *JAML* expression. Accordingly, we found minimal interactions between these gene loci in other immune cell types (i.e., B cells or monocytes) that lack active *CD3D* promoter regions, indicative of a T cell-specific *cis*-regulatory control of JAML expression (Figures 3B and S4A). As we have previously demonstrated that promoter-promoter interactions play a major role in regulating gene expression,[2] our data imply that the respective promoter regions of *CD3D* on the one hand, and *JAML* on the other hand, may act as reciprocal enhancers inducing each other's expression. TCR signaling is likely to increase NFAT binding and thus the transcriptional activity of the *CD3D* promoter, thus driving its own expression (Figure 3C) and with it, the expression of *JAML* through long-range *cis*-regulatory interactions. Together, these data demonstrate how and why *JAML* expression is induced in human T cells by TCR engagement and implies a T cell-specific inducible expression profile of this co-stimulatory molecule. Crucially and in line with our previous study,[4] these findings suggest that *JAML* expression might also be enriched in highly functional antigen-specific CD8$^+$ T_{RM} cells (i.e., reactive to tumor associated-antigens or neoantigens) driven by TCR-specific antigen-recognition and subsequent upregulation of *JAML* expression.

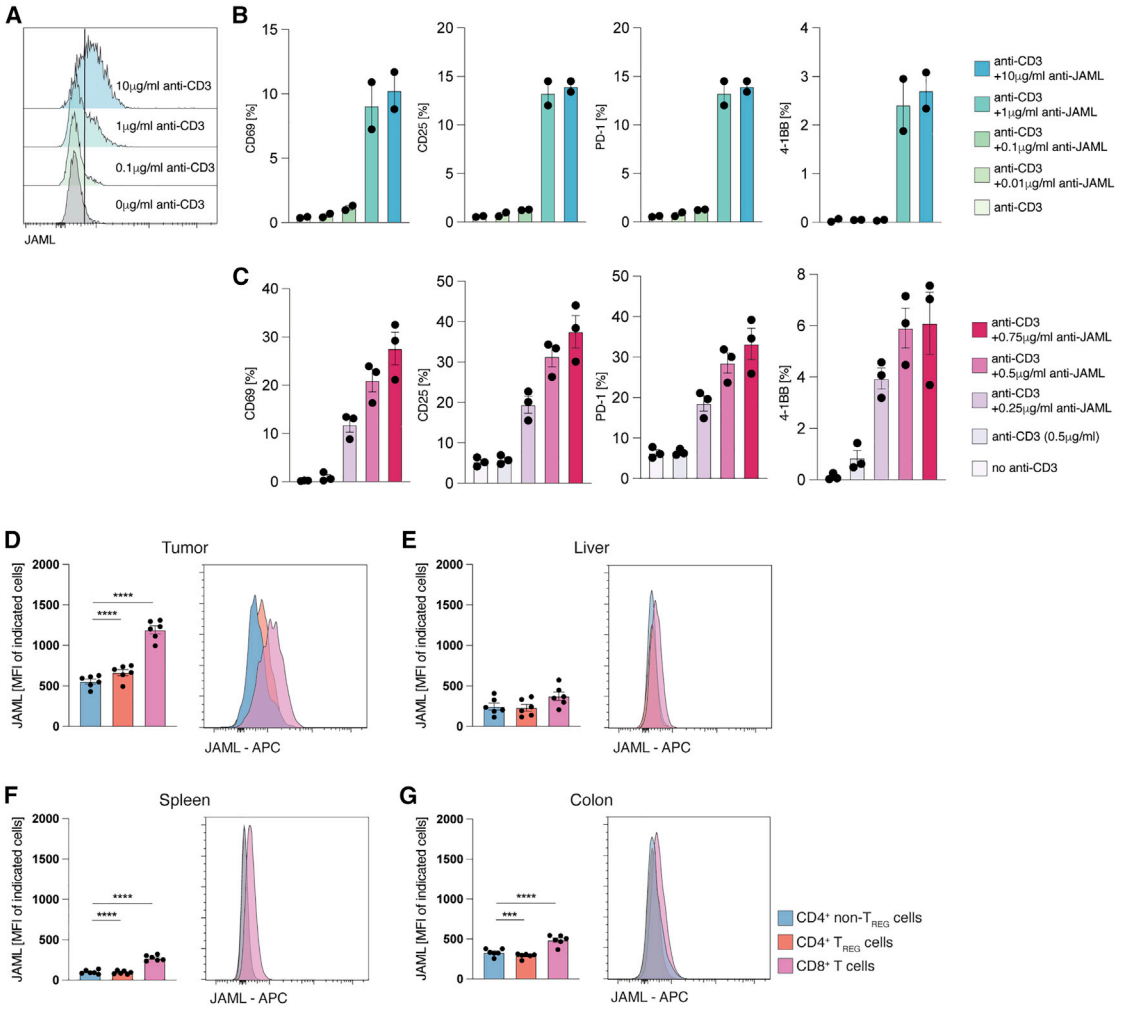

Figure 4. JAML is highly expressed by CD8$^+$ TILs in a murine melanoma model

(A) Representative histogram plots of *in vitro* stimulated CD8$^+$ T cells showing the expression levels of JAML in CD8$^+$ T cells treated as indicated.

(B and C) Flow-cytometric analysis of murine CD8$^+$ T cells stimulated with 0.1 μg/mL anti-CD3 + indicated concentrations of anti-JAML (B), or 0.5 μg/mL anti-CD3 + indicated concentrations of anti-JAML (C), depicted is the expression of early activation markers CD69, CD25, PD-1, and 4-1BB, results for n = 2 technical replicates are shown.

(D–G) Mice were subcutaneously inoculated with B16F10-OVA cells in the right flank. Flow-cytometric analysis and representative histogram plots of the MFI of JAML in T cell populations in indicated organs at day 18 after tumor inoculation (n = 6 mice/group), (tumor, $p < 0.0001$ for CD4$^+$ non-T_{REG} vs. CD8$^+$, $p < 0.0001$ for CD4$^+$ T_{REG} vs. CD8$^+$; spleen, $p < 0.0001$ for CD4$^+$ non-T_{REG} vs. CD8$^+$, $p < 0.0001$ for CD4$^+$ T_{REG} vs. CD8$^+$; colon, $p = 0.0002$ for CD4$^+$ non-T_{REG} vs. CD8$^+$, $p < 0.0001$ for CD4$^+$ T_{REG} vs. CD8$^+$). Data are mean ± SEM and are representative of at least two independent experiments. Significance for comparisons (D–G) was computed using one-way ANOVA comparing the mean of each group with the mean of the other groups followed by Tukey's test; $p = 0.1234$; *$p = 0.0332$; **$p = 0.0021$; ***$p = 0.0002$; and ****$p < 0.0001$.

Murine CD8$^+$ TILs selectively express high levels of JAML

We next assessed whether our findings in human T cells are also applicable to murine T cells. Similar to human αβ T cells, we found that TCR signaling rapidly upregulated JAML expression on murine αβ CD8$^+$ T cells (Figure 4A). Upon co-stimulation with an agonistic anti-JAML antibody[20] and anti-CD3, we observed a substantial upregulation of surface activation markers, confirming that JAML can function as a co-stimulatory molecule even in murine αβ T cells, a finding replicated in a recent study[21] (Figures 4B, S5A, and S5B). Importantly, stronger TCR stimulation resulted in higher expression of JAML and thus required an ~10-fold lower concentration of agonistic anti-JAML antibody to activate CD8$^+$ T cells even more strongly (Figure 4C), implying that high avidity T cells (i.e., tumor antigen-reactive CD8$^+$ T cells) expressing high levels of JAML, are likely to be highly sensitive to agonistic anti-JAML antibody treatment, even at relatively low concentrations. These results supported the rationale for testing the co-stimulatory function of JAML *in vivo*, especially in the context of tumor models, to determine if JAML could be used as a cancer immunotherapy target that potentially surpasses treatment efficacy of current immunotherapy drugs due to its

low expression on immunosuppressive T_{REG} cells. We tested this hypothesis in a murine melanoma model that is refractory to anti-PD-1 therapy. Given that short-term subcutaneous syngeneic tumor models do not induce robust anti-tumor $CD8^+$ T_{RM} responses,[26] we first assessed JAML expression levels on $CD4^+$ (T_{REG} and non-T_{REG}) and $CD8^+$ TILs of B16F10-OVA tumor-bearing mice. Consistent with our observations in human TILs, JAML was expressed at significantly higher levels in tumor-infiltrating $CD8^+$ T cells when compared with tumor-infiltrating T_{REG} cells and $CD4^+$ non-T_{REG} cells (Figure 4D), implying that treatment with agonistic JAML antibodies should preferentially activate $CD8^+$ T cells over immunosuppressive T_{REG} cells and thus enhance anti-tumor immune responses. Importantly, we found relatively low expression of JAML in $CD4^+$ and $CD8^+$ T cells present in spleen, colon, and liver of tumor-bearing mice (Figures 4E–4G), suggesting that therapies activating JAML are likely to act primarily on $CD8^+$ T cells within the tumor microenvironment (TME) and might therefore exert a favorable safety profile by not engaging T cells at common sites of immune-related toxicity. We further corroborated that notion by assessing the expression of JAML on bona fide small intestine intra-epithelial (siIEL) and lamina propria (LPL) T_{RM} cells, demonstrating that these cells do not express JAML under steady-state conditions (Figure S5C).

"Stem-like" CD8⁺ TILs express JAML

To determine the properties of tumor-infiltrating $CD8^+$ T cell subsets that express JAML and to explore the other immune cell types that express JAML in an unbiased manner, we performed single-cell RNA-seq of JAML-expressing $CD45^+$ cells present in primary late-stage tumor tissue of three individual B16F10-OVA tumor-bearing mice (Figure S5D). Unbiased clustering depicted by UMAP analysis revealed six clusters, and importantly, substantiated that JAML expression in the T cell compartment is restricted to $CD8^+$ TILs (cluster 0,2; Figure 5A). The JAML-expressing $CD8^+$ TILs (Figure 5B) clustered into two distinct subsets that displayed striking differences in the expression of transcripts encoding for TCF1 (*Tcf7*) and PD-1 (*Pdcd1*) (Figures 5C and 5D). We corroborated these data on the protein level, demonstrating that only a small proportion of TCF1-expressing $CD8^+$ T cells co-expressed PD-1 (Figure 5E), implying that anti-PD-1 treatment does not activate stem-like $CD8^+$ T cells in the TME. Conversely, we found similar ratios of JAML-expressing $CD8^+$ T expressing PD-1 or TCF1 (Figure 5E), suggesting that anti-JAML treatment might induce a sustained anti-tumor immune response as it would activate both stem-like and effector $CD8^+$ T cells. Furthermore, JAML-expressing and PD-1 expressing $CD8^+$ T cells also expressed high levels of CX3CR1, but not KLRG1 (Figure S5E), implying that such cells are a mixture of T_{CM}, T_{EM}, and stem-like T cells. The *Pdcd1*-low cluster (cluster 0) expressed high levels of molecules linked to "stem-like" properties (i.e., *Tcf7, Lef1, Cd5*), which have been shown to be important for sustaining anti-viral and anti-tumor immune responses[27–29] (Figures 5F and 5G). In contrast, the *Pdcd1*-enriched $CD8^+$ T cell cluster (cluster 2), when compared with cluster 0 $CD8^+$ T cells, displayed significantly higher expression of several transcripts linked to T cell activation (*Tnfrsf9, Pik3cd*), cytotoxicity (*Gzmb*, *Prf1*, *Ifng*), and cell proliferation (*Mki67*, *Top2a*), which suggested recent TCR activation by antigen encounter, presumably directed to tumor antigens. The *Pdcd1*-enriched cluster also expressed high levels of other transcripts linked to exhaustion (*Lag3*, *Havcr2*, *Tox*) (Figures 5B–5G), and in agreement with previous studies,[30,31] these results indicate that expression of these exhaustion-like markers in murine TILs is unlikely to impede their functionality. Instead, it appears that expression of these molecules is a necessary adaptation to survive in the TME[32] and to potentially limit immunopathology,[33] and likely marks effector T cells potentially responding to tumor antigens. Thus, these $CD8^+$ T cells by virtue of co-expressing both PD-1 and JAML are likely to be activated by both agonistic anti-JAML antibodies and anti-PD1 therapies, and, importantly, when these therapies are combined, synergistic activation and enhanced anti-tumor responses are likely. Whereas, JAML-expressing PD-1^- cells, which comprise stem-like T cells, are likely to be preferentially activated by agonistic anti-JAML antibodies when compared with anti-PD1 therapies. Sub-clustering of the *Jaml*-expressing $CD8^+$ T cell clusters combined with trajectory analyses revealed three distinct populations (two effector-like clusters and one stem-like cluster) and a developmental path originating from the stem-like *Tcf7*-expressing population, implying that these cells sustain the intratumoral effector pool (Figures 5H and 5I).

Although, other lymphocyte subsets like T_{REG} were not represented in JAML-expressing immune cells, we found several dendritic cell subsets expressed JAML (clusters 1, 4, 5) and corroborated previous reports of JAML-expressing neutrophils or granulocyte-derived myeloid-derived suppressor cells MDSCs (cluster 3),[34,35] (Figures 5A, 5B, and 5F) in the TME. This result suggests that therapies targeting JAML may have "on-target/off-cell" effects on JAML-expressing myeloid and dendritic cell compartments, but whether JAML agonistic antibodies modulate the functional activity of such cells remains to be explored. Conversely, anti-JAML antibodies are unlikely to elicit "on-target/off-tumor" effects, as T cells in other non-malignant organs lack substantial expression of JAML, and are thus unlikely to cause end-organ toxicity.

The anti-tumor effects of anti-JAML depend on $CD8^+$ TILs

In line with previous studies,[36] we found no changes in tumor volume upon anti-PD-1 monotherapy in the B16F10-OVA tumor model (Figure 6A). Conversely, treatment with agonistic anti-JAML antibodies significantly reduced tumor volume in B16F10-OVA tumor-bearing wild-type (Figure 6A), but not $CD8^{-/-}$ mice (Figure 6B), implying that the observed effects are likely dependent on $CD8^+$ T cells. Accordingly, while adoptive transfer of OVA antigen-specific JAML-sufficient OT-I $CD8^+$ T cells (OT-I $JAML^{wt}$) decreased tumor growth, CRISPR-Cas9-mediated depletion of JAML on transferred OT-I $CD8^+$ T cells (OT-I $JAML^{-/-}$) reduced tumor control (Figures 6C and S6A). Given that the frequencies of JAML-sufficient and JAML-deficient OT-I T cells in tumor tissues were comparable (Figure 6D), it is unlikely that the observed differences in tumor control can be contributed to distinct migration tendencies or altered *in vivo* persistence. These data imply that CXADR (endogenous JAML ligand) might be expressed by cells in the TME, as JAML-expressing, but not JAML-deficient OT-I

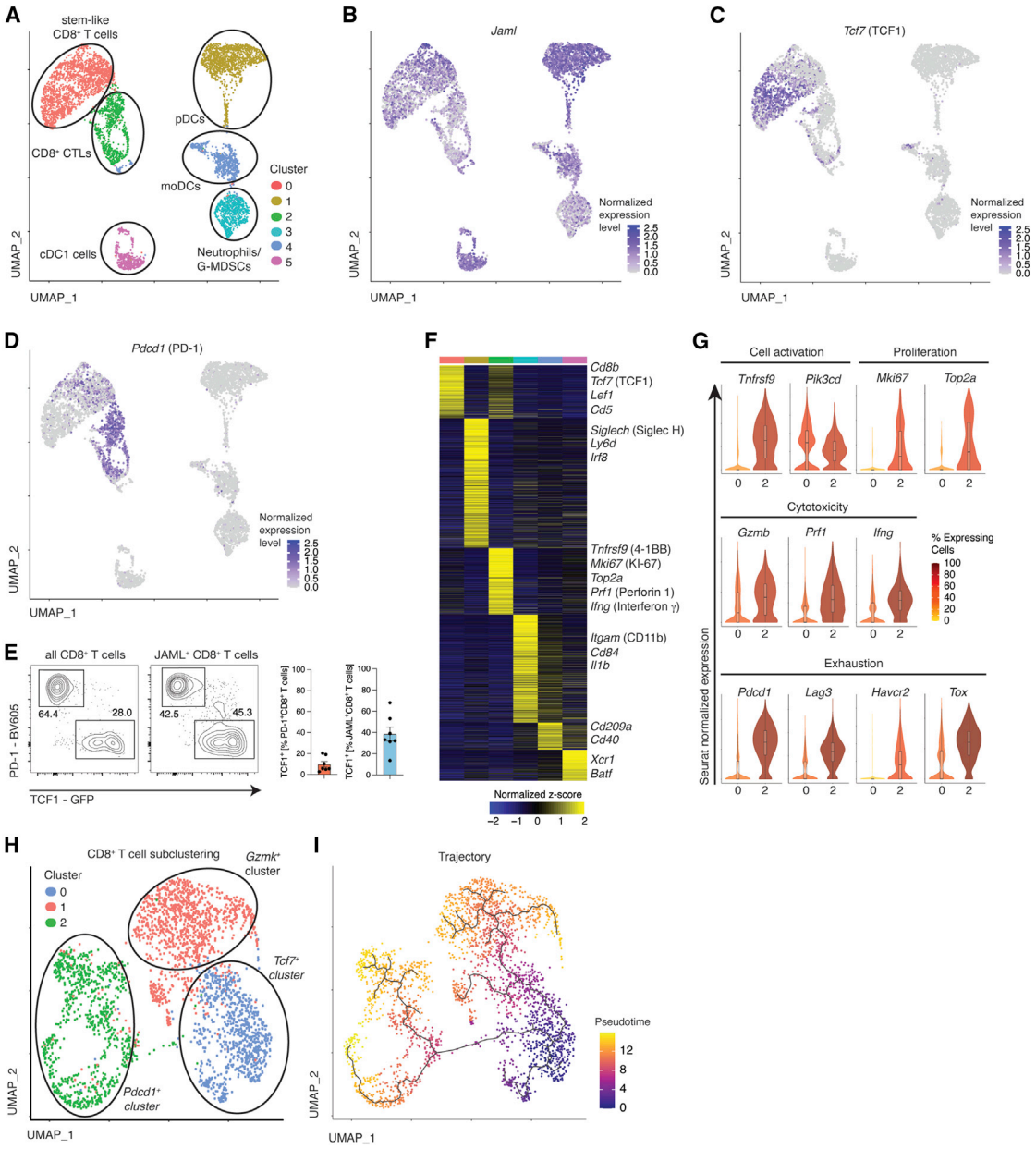

Figure 5. JAML is expressed by distinct CD8$^+$ TILs

(A–D) Analysis of 10x single-cell RNA-seq data visualized by UMAP. Seurat clustering of tumor-infiltrating CD45$^+$JAML$^+$ cells in the B16F10-OVA model at day 18 after tumor inoculation (A), (B–D) Seurat-normalized expression of *Jaml* (B), *Tcf7* (C), and *Pdcd1* (D).

(E) Flow-cytometric analysis of CD8$^+$ TILs (as in A) expressing the indicated markers.

(F) Heatmap depicting genes enriched in the identified clusters. Shown are significantly differentially expressed transcripts (Log2 FC > 0.25 and adjusted p value <0.05).

(G) Violin plots showing Seurat-normalized expression levels of the indicated markers in cells from cluster 0 and cluster 2.

(H) Sub-clustering of *Cd8*-expressing TIL subsets from (A).

(I) Single-cell pseudotime trajectory analysis of the subclustered CD8$^+$ TILs (H) constructed using the Monocle3 algorithm.

T cells, controlled tumor growth. Interestingly, we found that B16F10 melanoma cells expressed CXADR, albeit at profoundly lower levels when compared with MC38 adenocarcinoma cells (Figure S6B), implying that tumor cells might provide co-stimulation to JAML-expressing TILs. To test this hypothesis, we used CRISPR-Cas9 to generate CXADR-deficient MC38-OVA cells (Figure S6C) and performed an *in vitro* proliferation assay co-culturing either CXADR-sufficient or CXADR-deficient MC38-OVA tumor cells with CD8$^+$ OT-I T cells. Notably, we found significantly less proliferation of CD8$^+$ OT-I T cells when they

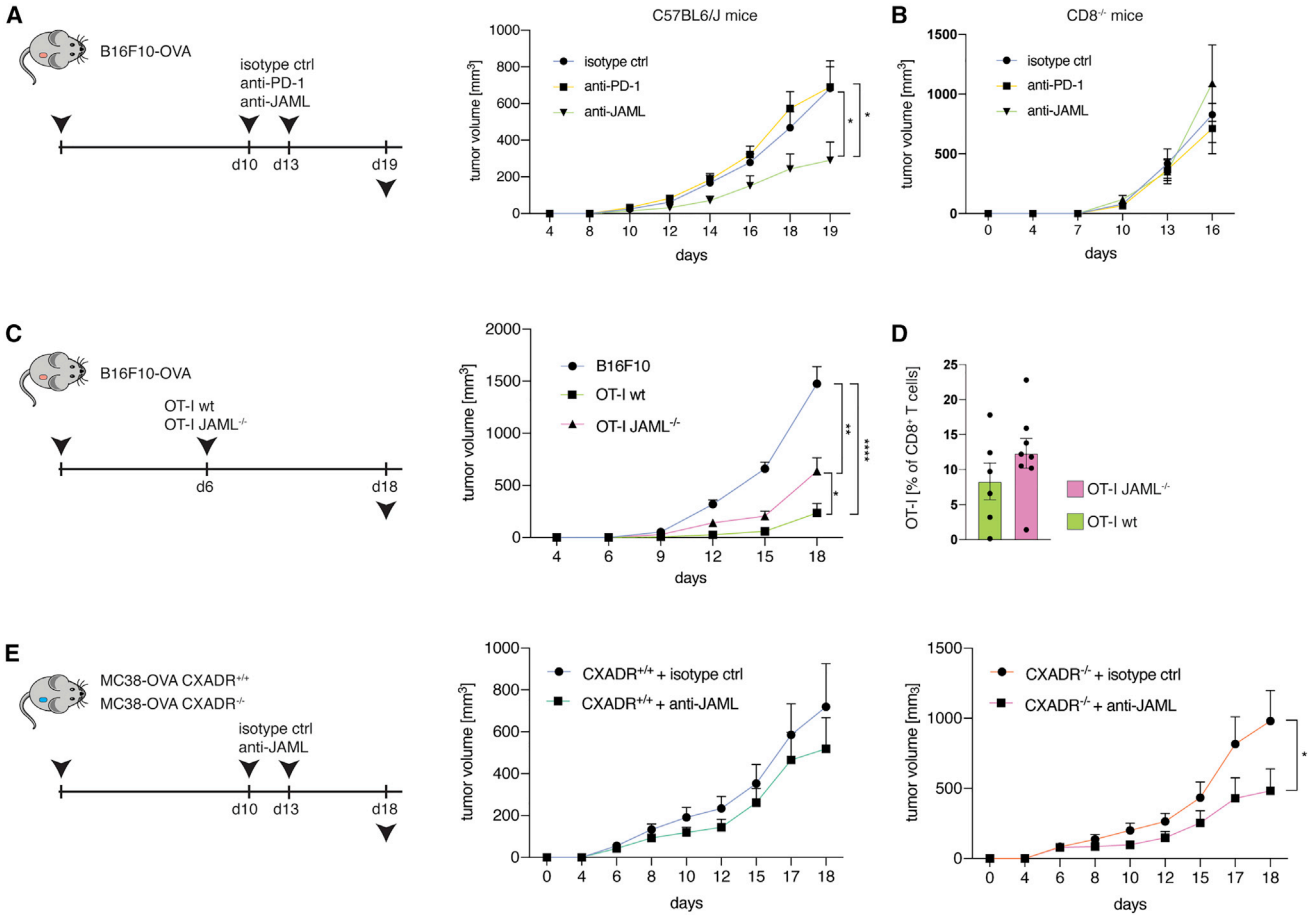

Figure 6. Agonistic JAML antibody treatment impedes tumor growth

(A and B) Tumor volume of C57BL/6J (A, n = 10 mice for isotype control group and n = 9 for anti-PD-1 and anti-JAML groups, p = 0.0141 for isotype control vs anti-JAML, and p = 0.0227 for anti-PD-1 vs anti-JAML) or CD8$^{-/-}$ (B, n = 7 mice/group for isotype control and anti-JAML and n = 6 mice/group for anti-PD-1) mice subcutaneously inoculated with B16F10-OVA cells and treated with isotype control antibodies, anti-PD-1 antibodies or anti-JAML antibodies at indicated time points.

(C and D) Tumor volume (C, p < 0.0001 for B16F10 vs. OT-I^{wt}, p = 0.0014 for B16F10 vs. OT-I JAML$^{-/-}$, p = 0.033 for OT-I^{wt} vs. OT-I JAML$^{-/-}$) (n = 13 mice/group for the control group, n = 8 mice/group for OT-I^{wt}, and n = 10 mice/group for OT-I JAML$^{-/-}$), and frequencies of tumor-infiltrating OT-I T cells (D, n = 6 mice/group for OT-I^{wt} and n = 8 mice/group for OT-I JAML$^{-/-}$) of mice subcutaneously inoculated with B16F10-OVA cells and treated with 1 × 10^6 adoptively transferred wild-type OT-I T cells or JAML$^{-/-}$ OT-I T cells at day 6 after tumor inoculation.

(E) Tumor volume of mice subcutaneously inoculated with CXADR$^{+/+}$ or CXADR$^{-/-}$ MC38-OVA cells and treated with either isotype control antibodies or anti-JAML antibodies at indicated time points (n = 8 mice/group for CXADR$^{+/+}$ + isotype control and n = 7 mice/group for CXADR$^{+/+}$ + anti-JAML, p = 0.61; n = 8 mice/group for CXADR$^{-/-}$ + isotype control and n = 7 mice/group for CXADR$^{-/-}$ + anti-JAML, p = 0.041). All data are mean ± SEM and are representative of at least two independent experiments. Significance for comparisons was computed using two-tailed Mann-Whitney test; *p < 0.05, **p < 0.01, ***p < 0.001, and ****p < 0.0001.

were co-cultured with CXADR$^{-/-}$ MC38-OVA tumor cells (Figure S6D), implying that tumor cells can provide co-stimulatory signals to CD8$^+$ TILs via CXADR. As we observed that agonistic anti-JAML antibody treatment decreased tumor growth in B16F10-OVA melanoma cells but not MC38-OVA tumor cells (Figures 6A and 6E), we reasoned that the disparate CXADR expression levels might be a critical determinant of anti-JAML treatment efficacy. To assess this hypothesis, we inoculated mice with either CXADR$^{+/+}$ or CXADR$^{-/-}$ MC38-OVA cells and found that anti-JAML therapy was more effective in CXADR$^{-/-}$ MC38-OVA treated mice (Figure 6E), implying that tumor cells themselves trigger TIL activation via JAML. Using The Cancer Genome Atlas data, we verified the relatively lower expression of CXADR on melanoma samples when compared with other tumors of epithelial origins like esophageal, colonic, and lung cancer (Figure S6E), pointing to a possible immune evasion mechanism in melanoma and highlighting the potential benefit of agonistic anti-JAML antibody treatment specifically in human cancers expressing low levels of CXADR. Accordingly, CXADR expression on tumor cells might be used as an effective biomarker to predict efficacy of anti-JAML treatment efficacy.

Synergistic anti-tumor effects in combination therapy with anti-PD-1 and anti-JAML

To elucidate molecular pathways selectively influenced by JAML signaling and to delineate the responsiveness of distinct TIL

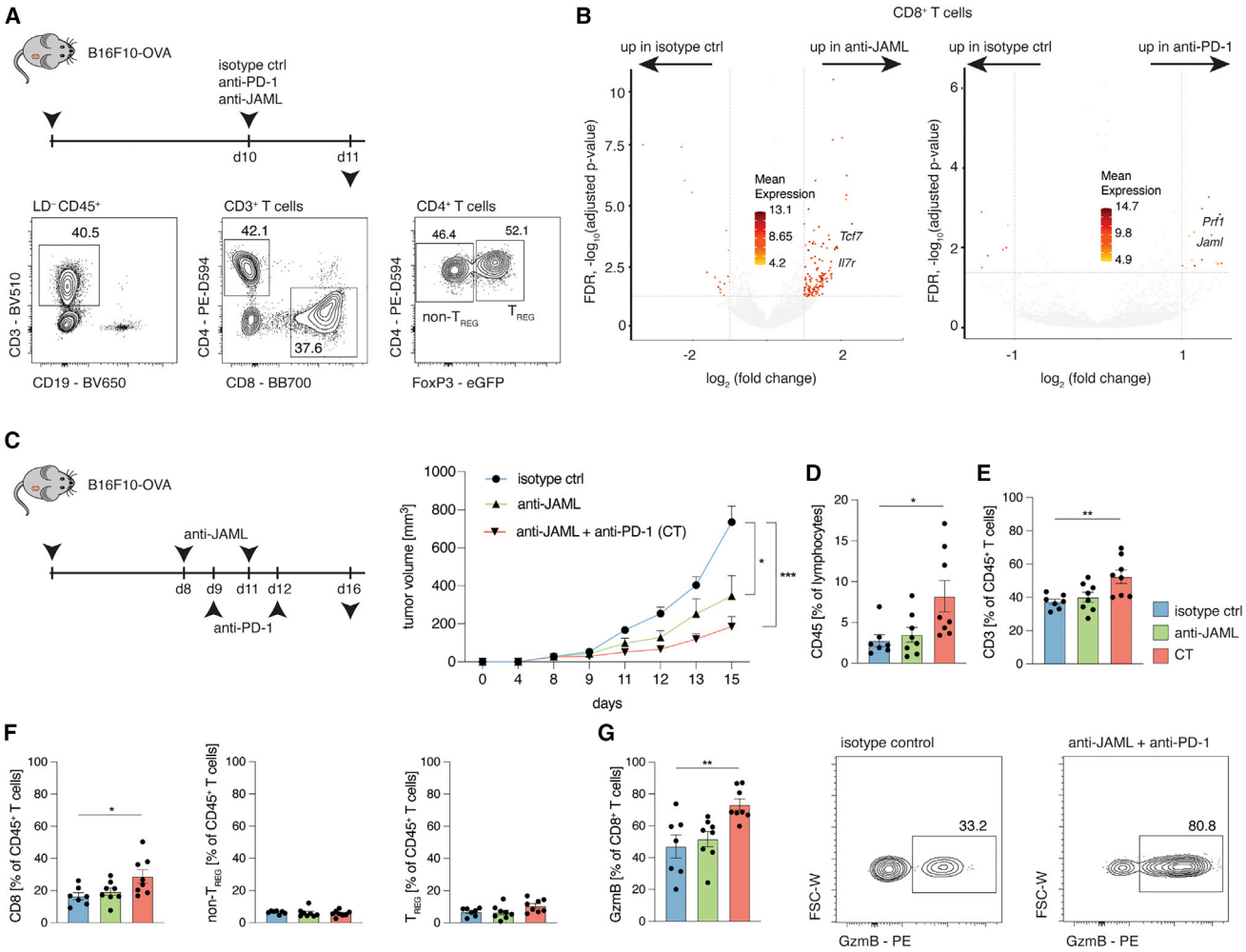

Figure 7. Anti-JAML synergizes with anti-PD-1 therapy

Mice were subcutaneously inoculated with B16F10-OVA cells or MC38-OVA in the right flank and treated with either isotype control antibodies, anti-PD-1 antibodies or anti-JAML antibodies at indicated time points.

(A) Representative histogram plots depicting the gating strategy for $CD4^+$ T_{REG} cells, $CD4^+$ non-T_{REG} cells and $CD8^+$ T cells.

(B) Volcano plot of isotype control vs anti-JAML (left) and isotype control vs anti-PD-1 (right) depicting differentially expressed transcripts (Log2 FC > 1 and adjusted p-value <0.05).

(C–G) Tumor volume (C, n = 7 mice/group for isotype control, n = 8 mice/group for anti-JAML and CT; p = 0.0225 for isotype control vs anti-JAML; p = 0.0006 for isotype control vs. CT), frequencies (D–G); p = 0.0192 (D), p = 0.0063 (E), p = 0.0211 (F), p = 0.0044 (G), and representative contour plots of indicated cell populations of B16F10-OVA tumor-bearing mice treated as indicated as in (C). Data (C–G) are mean ± SEM and are representative of at least two independent experiments. Significance for comparisons was computed using one-way ANOVA comparing the mean of each group with the mean of the control group (isotype control) followed by Dunnett's test; p = 0.1234; *p = 0.0332; **p = 0.0021; ***p = 0.0002; and ****p < 0.0001.

subsets to agonistic anti-JAML antibody and anti-PD1 treatment *in vivo*, we performed RNA-seq analyses of sorted tumor-infiltrating $CD4^+$ T_{REG} and $CD8^+$ T cells (Figure 7A). Pairwise comparison of the bulk transcriptomes of tumor-infiltrating $CD8^+$ T cells in treatment conditions versus isotype control showed that a greater number of genes were differentially expressed (DEG) in mice receiving agonistic anti-JAML therapy compared with anti-PD-1 therapy (151 versus 22 DEGs), and the converse was observed in tumor-infiltrating T_{REG} (45 versus 342 DEGs), (Figures 7B and S7A). In line with our previous study,[11] we found that anti-PD-1 therapy can activate suppressive T_{REG} cells, as evidenced by upregulation of several transcripts linked to functionality (*Prf1, Lag3*) and proliferation (*Mki67, Top2a*), while anti-JAML does not (Figure S7A).

These findings confirmed that unlike anti-PD-1 therapies, agonistic anti-JAML antibodies preferentially target $CD8^+$ TILs over immune-suppressive T_{REG} cells due to its restricted expression profile (Figure 7C). Importantly, anti-JAML treatment significantly increased the expression levels of genes (i.e., *Tcf7, Il7r*) shown to play a role in supporting "stem-like" properties of T cells,[27–29] implying that anti-JAML therapy might either maintain or reinforce the "stem-like" phenotype in tumor-infiltrating $CD8^+$ T cells (Figure 7B). This result supports our hypothesis, generated from single-cell transcriptomic analysis of

JAML-expressing CD8$^+$ TILs (Figures 5A–5G), that "stem-like" TILs are likely to be more responsive to agonistic anti-JAML antibodies when compared with anti-PD1 therapy.

Moreover, two of the most upregulated transcripts in CD8$^+$ T cells by anti-PD-1 therapy were *Prf1,* encoding for Perforin, and interestingly, *Jaml* (Figure 7B), indicative of an interconnected pathway between PD-1 signaling, which restricts TCR signaling and CD28 co-stimulation,[37,38] and JAML expression, which we found to be induced by TCR signaling. Thus, we hypothesize that releasing TCR restriction with anti-PD-1 antibodies upregulates the expression JAML on CD8$^+$ T cells, which can then be targeted by agonistic anti-JAML antibodies, causing a further and selective activation of (tumor antigen-specific) CD8$^+$ TILs. Based on these findings and given that anti-JAML agonistic antibody seems to reinforce a "stem-like" phenotype and as multiple studies have identified T_{SCM} cells as pivotal mediators of anti-PD-1 treatment efficacy,[27–29] we hypothesized that combination therapy (anti-JAML + anti-PD-1) is likely to result in improved tumor control. As before, we used the B16F10-OVA model that is refractory to anti-PD-1 monotherapy. Importantly, we found that anti-JAML/anti-PD-1 combination therapy resulted in greater reduction in tumor growth, demonstrating their synergistic effects (Figure 7C). This enhanced anti-tumor response was associated with a significant increase in TILs (Figure 7D), and was predominantly mediated by elevated levels of CD8$^+$ TILs, while the frequencies of CD4$^+$ non-T_{REG} or CD4$^+$ T_{REG} cells remained stable (Figures 7E and 7F). Notably, the proportion of granzyme B expressing CD8$^+$ TILs was also significantly higher in combination therapy compared with anti-JAML monotherapy or isotype controls (Figure 7G). Together, these findings provide mechanistic insights as to why agonistic anti-JAML therapy synergizes with anti-PD-1 treatment to improve tumor control.

DISCUSSION

Immunotherapies using agonistic antibodies were initially considered to mainly activate the CD8$^+$ T cell compartment, without appreciating potential effects on regulatory T cell subsets. However, subsequent studies have demonstrated that various immunotherapy drugs suffer from "on-target/off-cell effects" and "on-target/off-tumor effects," effectively dampening their treatment efficacy and clinical use. This initially underappreciated mechanism infers that T cell subsets other than CD8$^+$ T cells (i.e., suppressive T_{REG} or T_{FR} cells) can express high levels of a given immunotherapy drug target in tumor tissues (on-target/off-cell effects). By binding and activating such suppressive cells, immunotherapies can create an immunosuppressive milieu and thus impede clinical potential and utility. Contrary to that, an overactivation of the immune system in normal tissues (on-target/off-tumor effects), frequently observed by non-specifically targeting T_{REG} cells with anti-CTLA-4 and further exacerbated by combination with anti-PD-1 therapy, can cause severe irAEs. Hence, there remains an unmet need for the development of immunotherapy targets that exhibit a more restricted expression profile.

Here we show that the co-stimulatory molecule JAML is highly expressed in tumor-infiltrating CD8$^+$ T_{RM} cells in multiple human cancer types, and that its expression is associated with enhanced functional potential of T_{RM} cells and also improved long-term survival outcomes in a cohort of HNSCC patients. Using *in vitro* stimulation and CRISPR-Cas9 assays, we found that JAML signaling through its endogenous ligand CXADR potently and selectively activates CD8$^+$ T cells, and to a lesser degree, CD4$^+$ T cells. These assays also revealed that JAML is potently induced by TCR signaling, implying that antigen-recognition drives JAML expression. We demonstrated extensive 3D chromatin interactions between the promoters of *CD3D* and *JAML* in human T cells, but not other immune cell types like monocytes, implying that these *cis*-regulatory interactions might drive *JAML* expression. Crucially, these data suggest that agonistic anti-JAML antibodies might preferentially target and co-stimulate tumor antigen-specific CD8$^+$ T cells, which upregulated JAML expression due to recent TCR engagement, in tumor tissues. Accordingly, anti-JAML therapy showed beneficial effects in a murine melanoma model, an effect that was dependent on CD8$^+$ T cells. Moreover, we found JAML expression to be predominantly restricted to CD8$^+$ T cells in tumor tissue, with low expression in T cells from other organs or other T cell compartments, further substantiating the notion that it might specifically activate (antigen-specific) CD8$^+$ T cells in the TME, thus reducing the risk of irAEs in non-malignant organs. Crucially, in murine tumors, we found two distinct subsets of JAML-expressing CD8$^+$ T cells: (1) a "stem-like" population of CD8$^+$ T cells expressing high levels of *Tcf7*, demonstrated to be pivotal for efficacious immune responses against viruses and tumors, and (2) a *Pdcd-1* enriched effector CTL cluster, likely driving anti-tumor effects. Furthermore, by uncovering an interconnected pathway between JAML and PD-1, our data provide mechanistic insights for the observed synergistic effects of anti-JAML and anti-PD-1 therapy, which significantly increased TIL infiltration and thus efficiently controlled tumor growth. While a recent study described JAML as a potential cancer immunotherapy target in mice,[21] our study provides critical insights into how anti-JAML agonistic antibody mediates its function and identify JAML as an immunotherapy target in tumor-infiltrating T_{RM} cells with a low risk of "off-cell" and "off-tumor" effects, features that are likely to enhance anti-tumor efficacy without causing significant irAEs in humans.

Limitations of the study

We demonstrate that JAML is an attractive immunotherapy target that might primarily activate tumor antigen-specific CD8$^+$ T cells. A major limitation of the study is the lack of JAML protein expression data on human TIL populations, as well as on T cell subsets in non-malignant organs. This is crucial for the assessment of potential irAEs and thus requires assessments in future studies.

STAR★METHODS

Detailed methods are provided in the online version of this paper and include the following:

- KEY RESOURCES TABLE
- RESOURCE AVAILABILITY

SUPPLEMENTAL INFORMATION

Supplemental information can be found online at https://doi.org/10.1016/j.celrep.2023.112040.

ACKNOWLEDGMENTS

This work was funded by a combination of institutional, philanthropic, and corporate support. We thank C. Kim, D. Hinz, and C. Dillingham for their assistance with cell sorting (FACS Aria Fusion Cell Sorter; grant no. S10 RR027366); H. Simon for assistance with library preparation, next-generation sequencing using an Illumina HiSeq 2500 (NIH grant no. S10OD016262) and NovaSeq6000 (grant no. S10OD025052-01). This work was supported by the William K. Bowes, Jr. Foundation (P.V.) and the Whitaker Foundation (C.H.O.) . The funders have no role in the study design, data collection and analysis, decision to publish, or preparation of the manuscript.

AUTHOR CONTRIBUTIONS

S.E., C.H.O., and P.V. conceived the work. S.E., A.W., H.S., Y.L., and M.M. performed experiments. S.E., C.R.-S., and V.C. analyzed data under the supervision of C.H.O. and P.V. M.E. performed the immunohistochemical analyses under the supervision of G.J.T. A.v.W. and S.J.C. analyzed the immunohistochemistry data with regard to the survival plots. S.E. wrote the first draft of the manuscript that was revised and edited by C.H.O. and P.V.

DECLARATION OF INTERESTS

The La Jolla Institute of Immunology has filed a patent "Methods for modulating an immune response to cancer or tumor cells" related to this work, and S.E., P.V., and C.H.O. are co-inventors on this patent.

INCLUSION AND DIVERSITY

We support inclusive, diverse, and equitable conduct of research.

Received: January 4, 2022
Revised: November 27, 2022
Accepted: January 12, 2023
Published: January 25, 2023

REFERENCES

1. Schmiedel, B.J., Singh, D., Madrigal, A., Valdovino-Gonzalez, A.G., White, B.M., Zapardiel-Gonzalo, J., Ha, B., Altay, G., Greenbaum, J.A., McVicker, G., et al. (2018). Impact of genetic polymorphisms on human immune cell gene expression. Cell *175*, 1701–1715.e16. https://doi.org/10.1016/j.cell.2018.10.022.

2. Chandra, V., Bhattacharyya, S., Schmiedel, B.J., Madrigal, A., Gonzalez-Colin, C., Fotsing, S., Crinklaw, A., Seumois, G., Mohammadi, P., Kronenberg, M., et al. (2021). Promoter-interacting expression quantitative trait loci are enriched for functional genetic variants. Nat. Genet. *53*, 110–119. https://doi.org/10.1038/s41588-020-00745-3.

3. Schmiedel, B.J., Rocha, J., Gonzalez-Colin, C., Bhattacharyya, S., Madrigal, A., Ottensmeier, C.H., Ay, F., Chandra, V., and Vijayanand, P. (2021). COVID-19 genetic risk variants are associated with expression of multiple genes in diverse immune cell types. Nat. Commun. *12*, 6760. https://doi.org/10.1038/s41467-021-26888-3.

4. Clarke, J., Panwar, B., Madrigal, A., Singh, D., Gujar, R., Wood, O., Chee, S.J., Eschweiler, S., King, E.V., Awad, A.S., et al. (2019). Single-cell transcriptomic analysis of tissue-resident memory T cells in human lung cancer. J. Exp. Med. *216*, 2128–2149. https://doi.org/10.1084/jem.20190249.

5. Wolf, Y., Anderson, A.C., and Kuchroo, V.K. (2020). TIM3 comes of age as an inhibitory receptor. Nat. Rev. Immunol. *20*, 173–185. https://doi.org/10.1038/s41577-019-0224-6.

6. Manieri, N.A., Chiang, E.Y., and Grogan, J.L. (2017). TIGIT: a key inhibitor of the cancer immunity cycle. Trends Immunol. *38*, 20–28. https://doi.org/10.1016/j.it.2016.10.002.

7. Wang, B., Zhang, W., Jankovic, V., Golubov, J., Poon, P., Oswald, E.M., Gurer, C., Wei, J., Ramos, I., Wu, Q., et al. (2018). Combination cancer immunotherapy targeting PD-1 and GITR can rescue CD8+ T cell dysfunction and maintain memory phenotype. Sci. Immunol. *3*, eaat7061. https://doi.org/10.1126/sciimmunol.aat7061.

8. Gao, J., Ward, J.F., Pettaway, C.A., Shi, L.Z., Subudhi, S.K., Vence, L.M., Zhao, H., Chen, J., Chen, H., Efstathiou, E., et al. (2017). VISTA is an inhibitory immune checkpoint that is increased after ipilimumab therapy in patients with prostate cancer. Nat. Med. *23*, 551–555. https://doi.org/10.1038/nm.4308.

9. Andrews, L.P., Somasundaram, A., Moskovitz, J.M., Szymczak-Workman, A.L., Liu, C., Cillo, A.R., Lin, H., Normolle, D.P., Moynihan, K.D., Taniuchi, I., et al. (2020). Resistance to PD1 blockade in the absence of metalloprotease-mediated LAG3 shedding. Sci. Immunol. *5*, eabc2728. https://doi.org/10.1126/sciimmunol.abc2728.

10. Soldevilla, M.M., Villanueva, H., Meraviglia-Crivelli, D., Menon, A.P., Ruiz, M., Cebollero, J., Villalba, M., Moreno, B., Lozano, T., Llopiz, D., et al. (2019). ICOS costimulation at the tumor site in combination with CTLA-4 blockade therapy elicits strong tumor immunity. Mol. Ther. *27*, 1878–1891. https://doi.org/10.1016/j.ymthe.2019.07.013.

11. Eschweiler, S., Clarke, J., Ramírez-Suástegui, C., Panwar, B., Madrigal, A., Chee, S.J., Karydis, I., Woo, E., Alzetani, A., Elsheikh, S., et al. (2021). Intratumoral follicular regulatory T cells curtail anti-PD-1 treatment efficacy. Nat. Immunol. *22*, 1052–1063. https://doi.org/10.1038/s41590-021-00958-6.

12. Kumagai, S., Togashi, Y., Kamada, T., Sugiyama, E., Nishinakamura, H., Takeuchi, Y., Vitaly, K., Itahashi, K., Maeda, Y., Matsui, S., et al. (2020). The PD-1 expression balance between effector and regulatory T cells predicts the clinical efficacy of PD-1 blockade therapies. Nat. Immunol. *21*, 1346–1358. https://doi.org/10.1038/s41590-020-0769-3.

13. Ganesan, A.-P., Clarke, J., Wood, O., Garrido-Martin, E.M., Chee, S.J., Mellows, T., Samaniego-Castruita, D., Singh, D., Seumois, G., Alzetani, A., et al. (2017). Tissue-resident memory features are linked to the magnitude of cytotoxic T cell responses in human lung cancer. Nat. Immunol. *18*, 940–950. https://doi.org/10.1038/ni.3775.

14. Savas, P., Virassamy, B., Ye, C., Salim, A., Mintoff, C.P., Caramia, F., Salgado, R., Byrne, D.J., Teo, Z.L., Dushyanthen, S., et al. (2018). Single-cell profiling of breast cancer T cells reveals a tissue-resident memory subset associated with improved prognosis. Nat. Med. *24*, 986–993. https://doi.org/10.1038/s41591-018-0078-7.

15. Okła, K., Farber, D.L., and Zou, W. (2021). Tissue-resident memory T cells in tumor immunity and immunotherapy. J. Exp. Med. *218*, e20201605. https://doi.org/10.1084/jem.20201605.

16. Simoni, Y., Becht, E., Fehlings, M., Loh, C.Y., Koo, S.-L., Teng, K.W.W., Yeong, J.P.S., Nahar, R., Zhang, T., Kared, H., et al. (2018). Bystander CD8+ T cells are abundant and phenotypically distinct in human tumour infiltrates. Nature *557*, 575–579. https://doi.org/10.1038/s41586-018-0130-2.

17. Pardoll, D.M. (2012). The blockade of immune checkpoints in cancer immunotherapy. Nat. Rev. Cancer *12*, 252–264. https://doi.org/10.1038/nrc3239.

18. Hellmann, M.D., Ciuleanu, T.-E., Pluzanski, A., Lee, J.S., Otterson, G.A., Audigier-Valette, C., Minenza, E., Linardou, H., Burgers, S., Salman, P., et al. (2018). Nivolumab plus ipilimumab in lung cancer with a high tumor mutational burden. N. Engl. J. Med. *378*, 2093–2104. https://doi.org/10.1056/NEJMoa1801946.

19. Verdino, P., Witherden, D.A., Havran, W.L., and Wilson, I.A. (2010). The molecular interaction of CAR and JAML recruits the central cell signal transducer PI3K. Science *329*, 1210–1214. https://doi.org/10.1126/science.1187996.

20. Witherden, D.A., Verdino, P., Rieder, S.E., Garijo, O., Mills, R.E., Teyton, L., Fischer, W.H., Wilson, I.A., and Havran, W.L. (2010). The junctional adhesion molecule JAML is a costimulatory receptor for epithelial γδ T cell activation. Science *329*, 1205–1210. https://doi.org/10.1126/science.1192698.

21. McGraw, J.M., Thelen, F., Hampton, E.N., Bruno, N.E., Young, T.S., Havran, W.L., and Witherden, D.A. (2021). JAML promotes CD8 and γδ T cell antitumor immunity and is a novel target for cancer immunotherapy. J. Exp. Med. *218*, e20202644. https://doi.org/10.1084/JEM.20202644.

22. Buchan, S.L., Dou, L., Remer, M., Booth, S.G., Dunn, S.N., Lai, C., Semmrich, M., Teige, I., Mårtensson, L., Penfold, C.A., et al. (2018). Antibodies to costimulatory receptor 4-1BB enhance anti-tumor immunity via T regulatory cell depletion and promotion of CD8 T cell effector function. Immunity *49*, 958–970.e7. https://doi.org/10.1016/j.immuni.2018.09.014.

23. Kamada, T., Togashi, Y., Tay, C., Ha, D., Sasaki, A., Nakamura, Y., Sato, E., Fukuoka, S., Tada, Y., Tanaka, A., et al. (2019). PD-1 + regulatory T cells amplified by PD-1 blockade promote hyperprogression of cancer. Proc. Natl. Acad. Sci. USA *116*, 9999–10008. https://doi.org/10.1073/pnas.1822001116.

24. Edwards, J., Wilmott, J.S., Madore, J., Gide, T.N., Quek, C., Tasker, A., Ferguson, A., Chen, J., Hewavisenti, R., Hersey, P., et al. (2018). CD103+ tumor-resident CD8+ T cells are associated with improved survival in immunotherapy-naïve melanoma patients and expand significantly during anti-PD-1 treatment. Clin. Cancer Res. *24*, 3036–3045. https://doi.org/10.1158/1078-0432.CCR-17-2257.

25. Park, S.L., Gebhardt, T., and Mackay, L.K. (2019). Tissue-resident memory T cells in cancer immunosurveillance. Trends Immunol. *40*, 735–747. https://doi.org/10.1016/j.it.2019.06.002.

26. Park, S.L., Buzzai, A., Rautela, J., Hor, J.L., Hochheiser, K., Effern, M., McBain, N., Wagner, T., Edwards, J., McConville, R., et al. (2019). Tissue-resident memory CD8+ T cells promote melanoma–immune equilibrium in skin. Nature *565*, 366–371. https://doi.org/10.1038/s41586-018-0812-9.

27. Im, S.J., Hashimoto, M., Gerner, M.Y., Lee, J., Kissick, H.T., Burger, M.C., Shan, Q., Hale, J.S., Lee, J., Nasti, T.H., et al. (2016). Defining CD8+ T cells that provide the proliferative burst after PD-1 therapy. Nature *537*, 417–421. https://doi.org/10.1038/nature19330.

28. Siddiqui, I., Schaeuble, K., Chennupati, V., Fuertes Marraco, S.A., Calderon-copete, S., Pais Ferreira, D., Carmona, S.J., Scarpellino, L., Gfeller, D., Pradervand, S., et al. (2019). Intratumoral Tcf1+PD-1+CD8+ T cells with stem-like properties promote tumor control in response to vaccination and checkpoint blockade immunotherapy. Immunity *50*, 195–211.e10. https://doi.org/10.1016/j.immuni.2018.12.021.

29. Sade-Feldman, M., Yizhak, K., Bjorgaard, S.L., Ray, J.P., de Boer, C.G., Jenkins, R.W., Lieb, D.J., Chen, J.H., Frederick, D.T., Barzily-Rokni, M., et al. (2018). Defining T cell states associated with response to checkpoint immunotherapy in melanoma. Cell *175*, 998–1013.e20. https://doi.org/10.1016/j.cell.2018.10.038.

30. Scott, A.C., Dündar, F., Zumbo, P., Chandran, S.S., Klebanoff, C.A., Shakiba, M., Trivedi, P., Menocal, L., Appleby, H., Camara, S., et al. (2019). TOX is a critical regulator of tumour-specific T cell differentiation. Nature *571*, 270–274. https://doi.org/10.1038/s41586-019-1324-y.

31. Bassez, A., Vos, H., Van Dyck, L., Floris, G., Arijs, I., Desmedt, C., Boeckx, B., Vanden Bempt, M., Nevelsteen, I., Lambein, K., et al. (2021). A single-cell map of intratumoral changes during anti-PD1 treatment of patients with breast cancer. Nat. Med. *27*, 820–832. https://doi.org/10.1038/s41591-021-01323-8.

32. Alfei, F., Kanev, K., Hofmann, M., Wu, M., Ghoneim, H.E., Roelli, P., Utzschneider, D.T., von Hoesslin, M., Cullen, J.G., Fan, Y., et al. (2019). TOX reinforces the phenotype and longevity of exhausted T cells in chronic viral infection. Nature *571*, 265–269. https://doi.org/10.1038/s41586-019-1326-9.

33. Wang, Z., Wang, S., Goplen, N.P., Li, C., Cheon, I.S., Dai, Q., Huang, S., Shan, J., Ma, C., Ye, Z., et al. (2019). PD-1hi CD8+ resident memory T cells balance immunity and fibrotic sequelae. Sci. Immunol. *4*, 1217. https://doi.org/10.1126/sciimmunol.aaw1217.

34. Weber, D.A., Sumagin, R., McCall, I.C., Leoni, G., Neumann, P.A., Andargachew, R., Brazil, J.C., Medina-Contreras, O., Denning, T.L., Nusrat, A., and Parkos, C.A. (2014). Neutrophil-derived JAML inhibits repair of intestinal epithelial injury during acute inflammation. Mucosal Immunol. *7*, 1221–1232. https://doi.org/10.1038/mi.2014.12.

35. Alshetaiwi, H., Pervolarakis, N., McIntyre, L.L., Ma, D., Nguyen, Q., Rath, J.A., Nee, K., Hernandez, G., Evans, K., Torosian, L., et al. (2020). Defining the emergence of myeloid-derived suppressor cells in breast cancer using single-cell transcriptomics. Sci. Immunol. *5*, 6017. https://doi.org/10.1126/sciimmunol.aay6017.

36. Kleffel, S., Posch, C., Barthel, S.R., Mueller, H., Schlapbach, C., Guenova, E., Elco, C.P., Lee, N., Juneja, V.R., Zhan, Q., et al. (2015). Melanoma cell-intrinsic PD-1 receptor functions promote tumor growth. Cell *162*, 1242–1256. https://doi.org/10.1016/j.cell.2015.08.052.

37. Kamphorst, A.O., Wieland, A., Nasti, T., Yang, S., Zhang, R., Barber, D.L., Konieczny, B.T., Daugherty, C.Z., Koenig, L., Yu, K., et al. (2017). Rescue of exhausted CD8 T cells by PD-1 – targeted therapies is CD28-dependent. Science *355*, 1423–1427. https://doi.org/10.1126/science.aaf0683.

38. Hui, E., Cheung, J., Zhu, J., Su, X., Taylor, M.J., Wallweber, H.A., Sasmal, D.K., Huang, J., Kim, J.M., Mellman, I., and Vale, R.D. (2017). The T cell costimulatory receptor CD28 is a primary target of PD-1 mediated inhibition. Science *355*, 1428–1433. https://doi.org/10.1126/science.aaf1292.

39. Eschweiler, S., Ramírez-Suástegui, C., Li, Y., King, E., Chudley, L., Thomas, J., Wood, O., von Witzleben, A., Jeffrey, D., McCann, K., et al. (2022). Intermittent PI3Kδ inhibition sustains anti-tumour immunity and curbs irAEs. Nature *605*, 741–746. https://doi.org/10.1038/s41586-022-04685-2.

40. Engel, I., Seumois, G., Chavez, L., Samaniego-Castruita, D., White, B., Chawla, A., Mock, D., Vijayanand, P., and Kronenberg, M. (2016). Innate-like functions of natural killer T cell subsets result from highly divergent gene programs. Nat. Immunol. *17*, 728–739. https://doi.org/10.1038/ni.3437.

41. Picelli, S., Faridani, O.R., Björklund, A.K., Winberg, G., Sagasser, S., and Sandberg, R. (2014). Full-length RNA-seq from single cells using Smart-seq2. Nat. Protoc. *9*, 171–181. https://doi.org/10.1038/nprot.2014.006.

42. Guo, X., Zhang, Y., Zheng, L., Zheng, C., Song, J., Zhang, Q., Kang, B., Liu, Z., Jin, L., Xing, R., et al. (2018). Global characterization of T cells in non-small-cell lung cancer by single-cell sequencing. Nat. Med. *24*, 978–985. https://doi.org/10.1038/s41591-018-0045-3.

43. Zheng, C., Zheng, L., Yoo, J.K., Guo, H., Zhang, Y., Guo, X., Kang, B., Hu, R., Huang, J.Y., Zhang, Q., et al. (2017). Landscape of infiltrating T cells in

liver cancer revealed by single-cell sequencing. Cell *169*, 1342–1356.e16. https://doi.org/10.1016/j.cell.2017.05.035.

44. Zhang, L., Yu, X., Zheng, L., Zhang, Y., Li, Y., Fang, Q., Gao, R., Kang, B., Zhang, Q., Huang, J.Y., et al. (2018). Lineage tracking reveals dynamic relationships of T cells in colorectal cancer. Nature *564*, 268–272. https://doi.org/10.1038/s41586-018-0694-x.

45. Puram, S.V., Tirosh, I., Parikh, A.S., Patel, A.P., Yizhak, K., Gillespie, S., Rodman, C., Luo, C.L., Mroz, E.A., Emerick, K.S., et al. (2017). Single-cell transcriptomic analysis of primary and metastatic tumor ecosystems in head and neck cancer. Cell *171*, 1611–1624.e24. https://doi.org/10.1016/j.cell.2017.10.044.

46. Jerby-Arnon, L., Shah, P., Cuoco, M.S., Rodman, C., Su, M.J., Melms, J.C., Leeson, R., Kanodia, A., Mei, S., Lin, J.R., et al. (2018). A cancer cell program promotes T cell exclusion and resistance to checkpoint blockade. Cell *175*, 984–997.e24. https://doi.org/10.1016/j.cell.2018.09.006.

47. Oh, D.Y., Kwek, S.S., Raju, S.S., Li, T., McCarthy, E., Chow, E., Aran, D., Ilano, A., Pai, C.C.S., Rancan, C., et al. (2020). Intratumoral CD4+ T cells mediate anti-tumor cytotoxicity in human bladder cancer. Cell *181*, 1612–1625.e13. https://doi.org/10.1016/j.cell.2020.05.017.

48. Zhang, L., Li, Z., Skrzypczynska, K.M., Fang, Q., Zhang, W., O'Brien, S.A., He, Y., Wang, L., Zhang, Q., Kim, A., et al. (2020). Single-cell analyses inform mechanisms of myeloid-targeted therapies in colon cancer. Cell *181*, 442–459.e29. https://doi.org/10.1016/J.CELL.2020.03.048.

49. Maynard, A., McCoach, C.E., Rotow, J.K., Harris, L., Haderk, F., Kerr, D.L., Yu, E.A., Schenk, E.L., Tan, W., Zee, A., et al. (2020). Therapy-induced evolution of human lung cancer revealed by single-cell RNA sequencing. Cell *182*, 1232–1251.e22. https://doi.org/10.1016/J.CELL.2020.07.017.

50. Stuart, T., Butler, A., Hoffman, P., Hafemeister, C., Papalexi, E., Mauck, W.M., Hao, Y., Stoeckius, M., Smibert, P., and Satija, R. (2019). Comprehensive integration of single-cell data. Cell *177*, 1888–1902.e21. https://doi.org/10.1016/j.cell.2019.05.031.

51. Wolock, S.L., Lopez, R., and Klein, A.M. (2019). Scrublet: computational identification of cell doublets in single-cell transcriptomic data. Cell Syst. *8*, 281–291.e9. https://doi.org/10.1016/J.CELS.2018.11.005.

STAR★METHODS

KEY RESOURCES TABLE

REAGENT or RESOURCE	SOURCE	IDENTIFIER
Antibodies		
KLRG1 – BV421 (mouse)	Biolegend	Cat#138414; RRID: AB_2565613
CD3 – BV510 (mouse)	Biolegend	Cat#100353; RRID: AB_2565879
PD-1 – BV605 (mouse)	Biolegend	Cat#135220; RRID: AB_2562616
CD19 – BV650 (mouse)	Biolegend	Cat#115541; RRID: AB_11204087
CX3CR1 – BV711 (mouse)	Biolegend	Cat#149031; RRID: AB_2565939
FOXP3 – FITC (mouse)	eBioscience	Cat#11-5773-82; RRID: AB_465243
CD4 – PE-D594 (mouse)	Biolegend	Cat#100566; RRID: AB_2563685
CD8 – BB700 (mouse)	BD Biosciences	Cat#566409; RRID: AB_2744467
CD103 – BV421 (mouse)	Biolegend	Cat#121421; RRID: AB_2562901
JAML – APC (mouse)	Miltenyi	Cat#130-114-680; RRID: N/A
CD25 – BB700 (mouse)	BD Biosciences	Cat#566498; RRID: AB_2744345
4-1BB – PE (mouse)	Biolegend	Cat#106106; RRID: AB_2287565
CD69 – BV786 (mouse)	Biolegend	Cat#104543; RRID: AB_2629640
CXADR – A647 (mouse)	BEI Resources	NR-9216; RRID: N/A
ICOS – BV786 (human)	Biolegend	Cat#313534; RRID: AB_2629729
GITR – BV711 (human)	Biolegend	Cat#371212; RRID: AB_2687161
PD-1 – BV421 (human)	BD Biosciences	Cat#562584; RRID: AB_2737668
4-1BB – APC (human)	Biolegend	Cat#309810; RRID: A AB_830672
CD25 – PE (human)	BD Biosciences	Cat#555432; RRID: AB_395826
CD69 – BV605 (human)	Biolegend	Cat#310938; RRID: AB_2562307
Chemicals, peptides, and recombinant proteins		
CXADR Fc	R&D Systems	Cat#3336-CX-050 RRID: N/A
Deposited data		
Raw and analyzed data	This paper	GEO: GSE185162
Experimental models: Cell lines		
MC38-OVA	Peter MacCallum cancer center	N/A
B16F10-OVA	LJI	N/A
Experimental models: Organisms/strains		
C57BL/6J	Jackson Laboratories	#000664
OT-I	Jackson Laboratories	#003831
CD45.1	Jackson Laboratories	#002014
$CD8^{-/-}$	Jackson Laboratories	#002665
$TCF7^{GFP}$ flox	Jackson Laboratories	#030909
Software and algorithms		
Cell Ranger 3.1.0	10x Genomics	https://support.10xgenomics.com/single-cell-gene-expression/software/downloads/latest
bcl2fastq2 v2.20	illumina	https://support.illumina.com/sequencing/sequencing_software/bcl2fastq-conversion-software.html
Scrublet 0.2.3	Wolock et al.	https://github.com/swolock/scrublet
Seurat 3.1.5	Stuart et al.	https://github.com/satijalab/seurat

(*Continued on next page*)

Continued

REAGENT or RESOURCE	SOURCE	IDENTIFIER
Other		
Analysis code	This paper	https://github.com/vijaybioinfo/JAML_reproducibility

RESOURCE AVAILABILITY

Lead contact

Further information and requests should be directed to Pandurangan Vijayanand (vijay@lji.org).

Materials availability

This study did not generate new unique reagents.

Data and code availability

Expression data have been submitted to the Gene Expression Omnibus database (GSE185162, password: wtwdemycbdenpmz). This Super Series includes data from mouse samples. Source data are provided with this paper. H3K27ac ChIP-seq and HiChIP data for 6 common immune cell and ATAC-seq data for 15 DICE cell types have been previously reported[1,2,3] and are available from the database of Genotypes and Phenotypes (dbGaP; accession number: phs001703.v4.p1). ATAC-seq data for TRM cells and non-TRM cells were previously reported[4] and are available on GEO (accession number: GSE111898). NFATC1 and NFATC2 ChIP-seq data was obtained from GEO (accession number: GSM2810039 and GSM2810040 respectively). All original code has been deposited on GitHub (https://github.com/vijaybioinfo/JAML_reproducibility) and is publicly available as of the date of publication. An explanation and version changes are included. Any additional information required to reanalyze the data reported in this paper is available from the lead contact upon request.

EXPERIMENTAL MODEL AND SUBJECT DETAILS

C57BL/6J (stock no. 000664), OT-I (stock no. 003831). CD45.1 (stock no. 002014), $CD8^{-/-}$ (stock no. 002665) and $TCF7^{GFP}$ flox (stock no. 030909) mice were obtained from The Jackson Laboratory. In all experiments, female mice (6–12 weeks old) were used. In the vivarium, housing temperature was kept within the range of 20–24°C; humidity was monitored but not controlled and ranged from 30 to 70%. The mice were kept in 12h light–dark cycles (06:00–18:00 light). The La Jolla institute for Immunology Animal Ethics Committee approved all animal work.

METHOD DETAILS

Tumor cell lines

MC38-OVA cells, a gift from the S. Fuchs laboratory (UPenn) were approved for use by M. Smyth (Peter MacCallum cancer center). The B16F10-OVA cells were a gift from the J. Linden laboratory (LJI). All cell lines tested negative for mycoplasma infection and were subsequently treated with Plasmocin (InvivoGen) to prevent contamination.

Tumor models

Tumor models were used as described before.[11] The mice were s.c. inoculated with 2×10^6 MC38-OVA cells ($CXADR^{+/+}$ or $CXADR^{-/-}$) or 1–1.5 × 10^5 B16F10-OVA cells into the right flank. The mice were injected intraperitoneally at indicated time points with either 200μg isotype control antibodies, anti-PD-1 (29F1. A1, Bioxcell) or anti-JAML (4E10, Biolegend). Tumor size was monitored every 2–3 days to ensure that the tumors did not exceed 25mm in diameter. At experimental endpoint, tumors were harvested and tumor-infiltrating lymphocytes were analyzed. Tumor volume was calculated as described previously.[11]

CRISPR assays

Human or murine $CD8^+$ T cells were activated with 2 μg/mL of anti-CD3/anti-CD28 for 48h prior to electroporation and transfection with a pre-mixed sgRNA targeting JAML, CXADR or an irrelevant gene region using the Neon Transfection System (settings: 1,600V, 10ms, 3 pulses). Knockdown efficiency was evaluated via flow cytometry (murine) or real-time PCR (human) for transcripts. crRNA targeting murine *Jaml*: GGCCCTGTGGATAACCTACA, crRNA targeting murine *Cxadr*: ACGAGTAACGATGTCAAGTC, crRNA targeting human *JAML*: TGTCCCCCATCAAGTGTACG.

In vitro assays

$CD8^+$ T cells were labeled with CellTrace Violet (ThermoFisher). Subsequently, 20,000 cells were added to 96-well cell-culture plates containing 40,000 $CXADR^{+/+}$ or $CXADR^{-/-}$ cells respectively in 200μL complete RPMI medium. $CD8^+$ T cell proliferation was determined three days later. For detection of early activation markers, cells were stimulated with the indicated concentrations of anti-CD3, anti-JAML, anti-CD28 or recombinant CXADR Fc (chimeric fusion protein).

Flow cytometry

Lymphocytes were isolated from the liver or spleen by mechanically dispersing the cells through a 70μm cell strainer (Miltenyi) generating single-cell suspensions. RBC lysis (BioLegend) was performed to lyse and remove red blood cells. Tumors were harvested and TILs were isolated by dispersing the tumors in 2 mL sterile PBS and subsequently incubating the samples at 37°C with liberase DL (Roche) and DNase I (Sigma) for 15 min. Colonic tissue cell were isolated as described previously.[39] To create single-cell suspensions, the samples (tumor, liver, colon or spleen) were passed through a 70-μm cell strainer. The cells were kept in staining buffer (PBS with 2 mM EDTA and 2% FBS), FcγR blocked (clone 2.4G2, BD Biosciences), followed by staining with the indicated antibodies at 4°C for 30 min; secondary stains were conducted where indicated for selected markers. The samples were then either sorted or fixed and stained intracellularly with a FOXP3 transcription factor kit (eBioscience) according to the manufacturer's instructions. To determine cell viability, fixable viability dye (ThermoFisher) was used in all staining reactions. For the bulk RNA-seq analyses, we sorted tumor-infiltrating T_{REG} or $CD8^+$ cells based on the expression of the indicated markers (Figure 7A). All samples were sorted on a BD FACS Fusion system or acquired on a BD FACS Fortessa system (both BD Biosciences) and then analyzed using FlowJo 10.4.1. CXADR antibody was obtained through BEI Resources, NIAID, NIH: Monoclonal Anti-Mouse Coxsackie and Adenovirus Receptor, Clone U54.R.mCAR.4 (immunoglobulin G, Rat), NR-9216.

Histology and immunohistochemistry

The primary antibodies used for immunohistochemistry included anti-CD8 (pre-diluted; C8/144B, Agilent Dako), anti-JAML (1:100; Atlas, HPA047929), anti-CD103 (1:500; Abcam, ab129202), CK (1:5; Dako, AE1/AE3) The samples for the immunohistochemical analyses were prepared, stained and analyzed as previously described.[11] Cells were identified by nucleus detection and cytoplasmic regions were simulated up to 5 μm per cell; protein expression was measured using the mean staining intensity within the simulated cell regions.

Bulk RNA-seq

Total RNA was purified from murine tumor-infiltrating TREG ($LIN^-CD45^+CD3^+CD4^+FOXP3^+$) and $CD8^+$ T ($LIN^-CD45^+CD3^+CD8^+$) cells using the miRNeasy kit (Qiagen) and quantified as previously described.[13,40] RNA-seq libraries were prepared with a Smart-seq2 protocol and were sequenced on an Illumina platform.[41] Quality-control was applied as previously described[13] and data were analyzed as described previously.[11]

Meta-analysis of published single-cell RNA-seq studies

The meta-analysis was conducted as described previously.[11] In brief, nine published single-cell RNA-seq datasets[29,42–49] of CD4-expressing and CD8-expressing (n = 22,410) tumor-infiltrating T cells were integrated with UMAP using the R package Seurat v3.0. For each dataset, cells that expressed fewer than 200 genes were considered outliers and discarded. We integrated data from all cohorts using the alignment by the 'anchors' option in Seurat 3.0 as described previously.[11] Briefly, the alignment is a computational strategy to 'anchor' diverse datasets together, facilitating the integration and comparison of single-cell measurements from different technologies and modalities. The 'anchors' correspond to similar biological states between datasets. These pairwise correspondences between datasets allows the transformation of datasets into a shared space regardless of the existence of large technical and/or biological divergences. This improved function in Seurat 3.0 allows integration of multiple RNA-seq datasets generated by different platforms.[50] We used the FindIntegrationAnchors function to find correspondences across the different study datasets with default parameters (dimensionality = 1:30). Furthermore, we used the IntegrateData function to generate a Seurat Object with an integrated and batch-corrected expression matrix. In total, 22,410 cells and 2,000 most variable genes were used for clustering. We used the standard workflow from Seurat, scaling the integrated data, finding relevant components with principal-component analysis and visualizing the results with UMAP. The number of relevant components was determined from an elbow plot. UMAP dimensionality reduction and clustering were applied with the following parameters: 2,000 genes; 30 principal components; resolution, 0.4. The cells that were used for the integration were selected from clusters labeled in the original studies as tumor CD4+ T cells and from pretreatment samples when necessary.

Single-cell transcriptome analysis

Murine $CD45^+JAML^+$ cells from three B16F10-OVA tumor-bearing mice were isolated and prepared as described above. Cells from each mouse were barcoded with murine Totalseq-B antibodies. Cells were sorted and cDNA libraries were constructed using the standard 10x Genomics sequencing protocol. The antibody capture data were analyzed using custom scripts (github.com/vijaybioinfo/ab_capture), as previously described.[11] n = 8,474 cells were sequenced and doublets,[51] cells with fewer than 1,500 and more than 6,000 expressed genes, less than 1,000 and more than 50,000 counts, and more than 5% mitochondrial counts were

filtered out. 5,976 cells were used for downstream analyses. For clustering with Seurat (3.0), we used 15 principal components from a set of highly variable genes (n = 609) taking 20% of the variance after filtering out genes with a mean expression of less than 0.01. Differential gene expression was calculated using MAST ($p < 0.05$, $\log_2FC > 0.25$) as described previously.[11]

QUANTIFICATION AND STATISTICAL ANALYSIS

The number of mice per group and statistical tests used can be found in the figure legends. Details on sample elimination, quality control, and displayed data are stated in the figure legends and methods. Sample sizes were based on previous experiments and published studies to ensure reliable statistical testing accounting for variability between groups. Mice that did not develop tumors by 10 days after inoculation, before therapeutic intervention, were not included in the analyses. Low quality samples were excluded from the analyses and stated in the STAR Methods section. Data in heatmaps are displayed as $\log_2$-normalized z-scores. Experiments were reproduced in at least two independent experiments. Age and sex-matched mice were used in the experiments and animals were randomly assigned to the experimental groups. Statistical analyses were performed using GraphPad Prism 9. The graphical abstract has been created with Biorender.com.